Food Chemistry: X 21 (2024) 101184

Contents lists available at ScienceDirect

Food Chemistry: X

journal homepage: www.sciencedirect.com/journal/food-chemistry-x

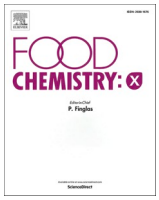

Influence of dextrans on the textural, rheological, and microstructural properties of acid-induced faba bean protein gels

Huihua Tang [a], Junfei Chen [a], Biqin Liu [a], Rong Tang [a], Hong Li [b], Xinyi Li [a], Ling Zou [c,*], Qiao Shi [a,*]

[a] Institute of Agro-Products Processing, Yunnan Academy of Agricultural Sciences, Kunming 65022, China
[b] College of Food Science and Technology, Yunnan Agricultural University, Kunming 650100, China
[c] Institute of Flower Research, Yunnan Academy of Agricultural Sciences, Kunming 650000, China

ARTICLE INFO

Keywords:
Faba bean protein
Dextran
Acid-induced gelation
Rheology
Microstructure

ABSTRACT

Dextrans (DXs) are a group of natural polysaccharides with different branching patterns. Previous studies examining the effects of DXs on plant protein gels have only focused on α-(1 → 3)-branched DXs. Here, we compared the effects of α-(1 → 3)-branched DX L12 with those of two α-(1 → 2)-branched DXs on the properties of glucono-δ-lactone-induced faba bean protein isolate (FPI) gels. DX L12 showed stronger effects in decreasing gel hardness and enhancing gel viscoelasticity than the other two DXs. Moreover, DX L12 decreased the water-holding capacity of FPI gels, whereas the other DXs enhanced it. Microstructural analysis revealed that DX addition promoted phase separation during gel formation. However, FPI/L12 gels exhibited greater phase separation than the other two gels and contained larger void spaces. These differences could be attributed to the varying water adsorption and self-association properties of the DXs. These findings could guide the application of DX in the tailored preparation of plant protein gels.

Introduction

The incorporation of plant proteins into food formulations for developing enriched food products has attracted growing interest in recent years. Faba bean, which has a protein content of approximately 29 % and a balanced amino acid profile, has the potential to serve as a good plant-derived protein source (Rahate et al., 2021). However, the utilization of this protein source remains limited, mainly due to the textural defects caused by its addition to foods. Several processing techniques have been developed to enhance the applicability of faba bean-derived ingredients (Augustin & Cole, 2022; Martineau-Côté et al., 2022). For example, fermentation with exopolysaccharide-producing lactic acid bacteria (LAB) can improve the properties of faba bean protein and flour, thereby increasing the sensory attributes of faba bean protein-enriched bread and pasta (Rizzello et al., 2019; Xu et al., 2017).

Protein gelation is essential for structure generation in a wide range of foods. Faba bean protein isolate (FPI) can form gels after heat treatment (Johansson et al., 2022), and gelation can also be induced by acid or salt after preheating-induced FPI denaturation. Acid-induced gelation can occur at lower protein concentrations and temperatures than heat-induced gelation (Zheng et al., 2019). Food acidification and subsequent protein gelation can often be achieved by culturing LAB and adding glucono-δ-lactone (GDL). The latter approach has been employed extensively to prepare plant protein gels as it allows easy modulation of the gelation process. Furthermore, GDL-induced gels are often used as a simplified model to study protein gelation during LAB fermentation (Pang et al., 2019).

The incorporation of polysaccharides has been demonstrated to improve the properties of GDL-induced plant protein gels (Monteiro et al., 2013). Dille et al. found that faba bean protein concentrate mixed with λ-carrageenan formed GDL-induced gels with acceptable mechanical properties. Moreover, in these gels, syneresis was found to decrease with increasing λ-carrageenan concentrations (Dille et al., 2022). Meanwhile, Lan et al. demonstrated that the addition of soybean soluble polysaccharides can have a profound impact on the gel properties and microstructure of GDL-induced soybean protein isolate gels (Lan et al., 2019).

Dextrans (DXs) are neutral non-gelling polysaccharides produced by LAB and are often employed as food thickeners and texture modifiers (Dong et al., 2022). DXs consist of D-glucose units linked by continuous

* Corresponding authors.
E-mail addresses: ling.zou.cn@outlook.com (L. Zou), sq@yaas.org.cn (Q. Shi).

https://doi.org/10.1016/j.fochx.2024.101184
Received 6 October 2023; Received in revised form 10 January 2024; Accepted 2 February 2024
Available online 5 February 2024
2590-1575/© 2024 The Author(s). Published by Elsevier Ltd. This is an open access article under the CC BY-NC-ND license (http://creativecommons.org/licenses/by-nc-nd/4.0/).

α-(1 → 6) linkages along with varied proportions of α-(1 → 2), α-(1 → 3), or α-(1 → 4) branch linkages. Typical DXs mainly contain α-(1 → 6) linkages and a low percentage of α-(1 → 3) branch linkages (Chen et al., 2019). Heat-induced FPI gels formed after the addition of two typical α-(1 → 3) branched DXs were examined in a previous study, and the findings showed that DXs can stabilize the protein network in these gels (Xu et al., 2018). However, the characteristics of FPI gels formed after the addition of DX with other branching patterns remain to be explored.

The aim of this study was to characterize the impact of DXs with different branching patterns on the properties of GDL-induced FPI gels. In addition to a typical α-(1 → 3) branched DX, two α-(1 → 2) branched DXs were prepared and mixed with FPI at a fixed concentration of 2 %. The physical properties and microstructures of the gels formed after GDL-induced gelation were examined. Furthermore, protein interaction force analysis and Fourier-transform infrared (FTIR) spectroscopy were conducted to better understand the mechanism underlying the effects of DXs. To the best of our knowledge, this is the first study to report the effects of different DXs on the properties of acid-induced FPI gels.

Materials and methods

Materials

The Yundou 1183 variety of dried faba bean (*Vicia faba* L.) was procured from the Food Crops Research Institute, Yunnan Academy of Agricultural Sciences. The three LAB strains used in this study (*Leuconostoc citreum* L12, *L. citreum* B12, and *L. citreum* G26) were preserved in the Food Microbial Culture Collection, Yunnan Academy of Agricultural Sciences. Chemicals of analytical grade were purchased from Sinopharm Chemical Reagent Co. Ltd. (China).

Faba bean protein isolate preparation

FPI was prepared using an alkaline extraction method with 1 M NaOH (pH 9.5) (Makri et al., 2006). The protein content of freeze-dried FPI was determined using the Dumas method, and a conversion factor of 6.25 was employed to convert nitrogen content into protein content (Serrano et al., 2013).

HYPERLINK "SPS:id::Sec1" Crude dextran preparation

Crude DXs were isolated from three *L. citreum* fermentation cultures. *L. citreum* strains were activated via static incubation in MRS liquid medium at 37 °C for two generations. The seed solution was inoculated into modified MRS broth (1 mL/100 mL) with sucrose (100 mg/mL) as the only carbon source and incubated for 48 h at 30 °C. Subsequently, the culture was centrifuged at 7000 × *g* and 4 °C for 10 min, and the supernatant was treated with trichloroacetic acid (final concentration of 50 mg/mL). The protein was then removed by stirring for 2 h and centrifuging at 7000 × *g* and 4 °C for 10 min. The supernatant obtained was precipitated using a triple volume of ethanol for 12 h and the mixture was centrifuged at 7000 × *g* for 10 min. The pellet was dialyzed against water using a biological semipermeable membrane (14 kDa molecular weight cut-off) and then freeze-dried. The weight-average molar mass (M_w) of DX was assessed using high-performance size-exclusion chromatography (Rid-20A, Shimatsu, Japan) (Maina et al., 2014). The composition of glycosidic linkages was characterized using Proton nuclear magnetic resonance spectroscopy (^{1}H NMR) (800 MHz, 25 °C, D_2O) (AVANCE III HD-800 MHz, Bruker, Switzerland) (Heperkan et al., 2020). Finally, the intrinsic viscosity of DX was determined using a capillary viscometer at 25 °C (Monteiro et al., 2013).

Preparation of GDL-induced FPI/DX gels

To determine the optimal formulation parameters for the FPI gel, different final FPI concentrations (60, 80, 100, 120 mg/mL) and GDL concentrations (5, 10, 20 mg/mL) were tested, and selection was based on visual examination (Brito-Oliveira et al., 2017). A minimum FPI concentration of 80 mg/mL in the presence of 10 mg/mL GDL provided adequate gel stability and was thus chosen for subsequent experiments. Then, in order to select the fixed DX concentration for the preparation of FPI/DX gels, different concentrations of DX from *L. citreum* B12 were tested (2.5, 5, 10, and 20 mg/mL). Eventually, a final DX concentration of 20 mg/mL was selected.

The FPI/DX mixed gels were prepared as described in our previous study, with slight modifications (Tang et al., 2023). Briefly, an FPI/DX mixture was obtained by dissolving FPI and DX powders in deionized water to achieve a final concentration of 80 mg/mL and 20 mg/mL, respectively. The FPI/DX solution was heated at 80 °C for 30 min, and then, the GDL solution was immediately added. After cooling, the mixture was incubated at 4 °C overnight to obtain the FPI/DX mixed gel. A portion of the FPI/DX gel samples was vacuum lyophilized for subsequent analysis. Notably, under the experimental conditions, the mixture of FPI (80 mg/mL) and DX (20 mg/mL) could not form a gel in the absence of GDL addition.

Gel hardness analysis

Gel hardness was measured using a texture analyzer (TMS-Touch, FTC, USA) equipped with a cylindrical probe (P/0.5R). The measurement was conducted at a constant speed of 2.0 mm/s using a trigger point load of 0.045 N and a compression depth of 4 mm. Hardness was defined as the peak force during the first compression cycle.

Water-holding capacity (WHC) analysis

Fresh gel samples (10 g) were centrifuged at 7000 × *g* and 25 °C for 10 min. WHC was expressed as the ratio of gel weight after decanting to that before centrifugation.

Dynamic rheological analysis

The frequency sweeps of the FPI/DX gels were measured using a HAAKE rotation rheometer (MARS40, Thermo Fisher, USA) and a pp50 plate (1-mm gap) at 25 °C. The storage modulus (G') and loss modulus (G") of the FPI gels were determined as a function of frequency (f) using the following parameters: strain, 1 %, within the linear viscoelastic region; and frequency range, 1–100 rad/s.

Confocal laser scanning microscopy (CLSM) analysis

The FPI/DX mixture was stained with 0.01 mg/mL Rhodamine B prior to heat treatment. After GDL addition as described in section 2.3, a small volume of the mixture was placed on a microscope glass slide and kept at 4 °C for 24 h to allow gel formation. CLSM was performed (Leica TCS SP8, Germany) using an excitation wavelength of 514 nm and an emission wavelength range of 551–655 nm, at 400 × magnification.

Analysis of chemical interaction

Various solvents were employed to assess protein solubility in order to elucidate the chemical interactions governing gel formation (Gómez-Guillén et al., 1997). Freeze-dried gels were dissolved in the following solvents at a concentration of 20 mg/mL: 0.05 mol/L NaCl (LA), 0.6 mol/L NaCl (LB), 0.6 mol/L NaCl + 1.5 mol/L urea (LC), 0.6 mol/L NaCl + 8 mol/L urea (LD), and 0.6 mol/L NaCl + 8 mol/L urea + 0.5 mol/L 2-mercaptoethanol (LE). The mixtures were vortexed for 1 h at 5 °C and then centrifuged at 7000 × *g* for 15 min. The protein concentration of the supernatant — expressed as g soluble protein/L of solution — was determined using the Bradford method. The driving molecular forces, i.e. ionic bonds, hydrogen bonds, hydrophobic interactions, and disulfide bonds, were estimated based on the differences in protein solubility

between LA and LB, LB and LC, LC and LD, and LD and LE, respectively.

Determination of free sulfhydryl group (SH-) content

The free sulfhydryl group content of FPI/DX gels was analyzed using Ellman's reagent (DTNB) (Beveridge et al., 1974). Briefly, 30 mg of the freeze-dried sample was suspended in 10.0 mL Tris-glycine buffer (pH 8.0), followed by the addition of 0.1 mL of 4 mg/mL DTNB. The mixture was incubated in the dark under constant stirring for 1 h and then centrifuged at 7000 × *g* for 10 min. The absorbance of the supernatant at 412 nm (A_{412}) was determined against a reagent blank using a microplate reader (Multiskan GO, Thermo Scientific, USA). SH- content was measured as follows:

$$SH-(\mu mol/g) = 73.53 \times A_{412} \times D/C \quad (1)$$

where D stands for the dilution coefficient and C (mg/mL) for the protein concentration in the tested sample.

Fourier-transform infrared spectroscopy

FTIR was used to analyze the functional groups in gel samples (Mu et al., 2020). Briefly, a small amount of freeze-dried sample was added to KBr and ground in an agate mortar. The mixture was then pressed into thin and transparent sheets using a tablet press, and the sheets were examined using an FTIR spectrometer (Nicolet iS50, Thermo Electron Corporation, USA) over a scanning wavelength range of 4000–400 cm^{-1}.

Data analysis

All experiments were performed in triplicate. Data were presented as the mean ± standard deviation (SD). SPSS 22.0 (IBM Inc., USA) was applied for analysis of variance (ANOVA). Differences among groups were considered significant at $P < 0.05$ based on the least significant difference (LSD) test. Origin 8.5 (Origin Lab Inc., USA) was used to plot all graphs.

Result and discussiwon

Characterization of crude DXs

The characteristics of crude DXs derived from the exopolysaccharides of three different *L. citreum* strains are shown in Table 1 and Fig. 1. The DXs had similar weight-average molecular weights, ranging from 10^6 to 10^7 g/mol. Based on the chemical shifts and intensities of anomeric proton signals, the DXs were mainly found to contain α-(1 → 6) glycosidic linkages and varied percentages of α-(1 → 3) or α-(1 → 2) linkages (Table 1). DX L12 had a typical α-(1 → 3)-branched structure, whereas DX B12 and DX G26 were α-(1 → 2)-branched and showed varied degrees of branching. Typically, in these types of α-(1 → 3)-branched DXs, the branches can be single glucosyl units or consist of one or more α-(1 → 6)-linked glucosyl residues (Maina et al., 2011; Xu et al., 2018). However, single-unit-branches were previously found to be characteristic of such α-(1 → 2)-branched DXs (Yang et al., 2015).

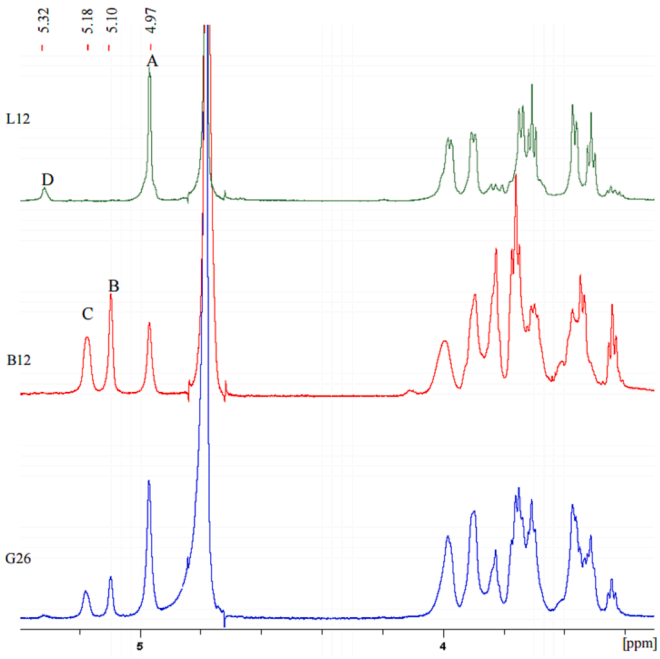

Fig. 1. ^{1}H NMR spectra of the DX isolates from the three *Leuconostoc* strains, namely, *L. citreum* L12, *L. citreum* B12, and *L. citreum* G26. Anomeric protons are labeled A–D in the increasing order of chemical shifts.

The intrinsic viscosity of a polysaccharide is a measure of the hydrodynamic volume of individual molecules in a solution and indicates their stretching state and conformation (Li et al., 2016). Polysaccharides with higher intrinsic viscosity generally interact well with the solvent, while those with lower intrinsic viscosity tend to exhibit tight conformations when dissolved (Spotti et al., 2019). As shown in Table 1, DX L12 had the lowest intrinsic viscosity, likely due to the presence of elongated branches, which resulted in a relatively tight conformation. The other two DXs with (1 → 2)-linked single-unit branches probably formed a comb-like shape, exhibited a more open conformation, and had a higher intrinsic viscosity. Thus, DXs with different macromolecular properties were employed to investigate the impact of DX supplementation on the properties of FPI gels.

Preparation of GDL-induced FPI gels

The freeze-dried FPI samples prepared in this study had a protein content of 83.75 g/100 g, which was acceptable for subsequent experiments. To prepare acid-induced gels, the FPI solution was pre-heated to cause protein denaturation and consequently allow the formation of soluble aggregates. While some gels were prepared with DX addition, others were not. The acidifying agent GDL was then added to the system to induce gel formation. In order to avoid heat-induced gel formation,

Table 1
Producer microorganisms, weight-average molar mass (M_w), intrinsic viscosity, and glucopyranosyl unit composition of the crude dextran samples.

DX samples	Producer microorganisms	M_w (g/mol)	Intrinsic viscosity (cm^3/g)	Constituent glucopyranosyl unit	Distribution (%)
L12	*L. citreum* L12	3.86×10^6	6.14	→6)-α-D-Glcp-(1 → 6)-(A)	87.79
				→3,6)-α-D-Glcp-(1 → 6)-(D)	12.21
B12	*L. citreum B12*	4.78×10^6	36.15	→6)-α-D-Glcp-(1 → 6)-(A)	34.39
				α-D-Glcp-(1 → 2)-(B)	33.57
				→2,6)-α-D-Glcp-(1 → 6)-(C)	32.04
G26	*L. citreum G26*	4.98×10^6	23.33	→6)-α-D-Glcp-(1 → 6)-(A)	68.56
				α-D-Glcp-(1 → 2)- (B)	15.50
				→2,6)-α-D-Glcp-(1 → 6)-(C)	15.94

(A)–(D) represent different types of glucopyranosyl units identified based on the anomeric proton signals in Fig. 1.

the minimum FPI concentration was first optimized in the presence of GDL. Visual examination revealed that self-supporting gels could only be formed when the concentrations of FPI and GDL were at least 80 mg/mL and 10 mg/mL, respectively. Below these critical thresholds, viscous dispersions or non-supported gels were obtained. Subsequently, optimal concentrations of DX were also screened for the preparation of mixed gels. The gel with the highest DX concentration (20 mg/mL) showed the highest WHC and rigidity based on the viscoelastic modulus G' after storage for 48 h. This was in line with our previous observation for a typical α-(1 → 3)-branched DX, where the highest level of supplementation (20 mg/mL) enabled the generation of a mixed FPI gel with desirable traits (Tang et al., 2023). Therefore, a DX concentration of 20 mg/mL was chosen to investigate the effects of DXs with different branching features on FPI gels. Mende et al. evaluated the impact of 5–30 g/kg DX on acid-induced milk gels and also found that an increase in DX concentration increases gel stiffness and stability (Mende et al., 2013).

Impact of DX supplementation on the physical properties of FPI gels

Hardness and WHC

Gel hardness is an important indicator of gel quality. In this study, DX addition was found to decrease the hardness of mixed gels (FPI gels vs. FPI/DX gels) (Table 2). Similarly, Ullah et al. demonstrated that adding dietary fiber could reduce tofu gel hardness by producing a more heterogeneous and unstable network structure (Ullah et al., 2019). Johansson et al. observed that fiber and starch granules can act as filler particles in mixed FPI gels and produce heterogeneity in the protein matrix, thereby reducing gel hardness (Johansson et al., 2022).

WHC is another important gel quality parameter, and it signifies the gel's capacity to immobilize water through capillary force. Moreover, WHC is also associated with the gel's matrix structure (Mende et al., 2020), and a low WHC generally indicates low textural stability (Zheng et al., 2019). As shown in Table 2, the addition of DXs with different macromolecular properties had different effects on the WHC of FPI gels. Notably, the WHC decreased when DX L12 was added. Pang et al. found that the addition of locust bean gum (0.1 %) causes a considerable reduction in the WHC of soymilk gels, and this change was attributed to depletion flocculation phenomena (Pang et al., 2020). Interestingly, the WHC increased from 61.23 g/100 g to 72.33 g/100 g when DX G26 was added. A similar trend was also observed for samples treated with DX B12. Zhao et al. revealed that the incorporation of starch in acid-induced soy protein gels could increase the WHC. They speculated that the presence of starch facilitates the uptake of water and the formation of a denser gel structure owing to the filling effect of starch, leading to enhanced water retention in the gel (Zhao et al., 2023).

Dynamic rheological analysis

The frequency dependence of mixed gels is presented in Fig. 2(A, B). Both the G′ and G″ values of the gels increased with increasing frequency, with G' being higher than G'' across the frequency range. The addition of DXs, especially DX L12, increased gel rigidity (versus FPI alone). Similar behaviors have been reported for other protein/polysaccharide gels, such as those made from egg white protein and DX (Mu et al., 2020), fiber and FPI (Johansson et al., 2022), and locust bean gum and soymilk (Pang et al., 2020). The viscoelastic properties of the mixed gels can be affected by the nature, conformation, and concentration of the polysaccharide, among other factors (Cortez-Trejo et al., 2021). Johansson et al. reported an increase in the G' of FPI gel following the addition of starch/fiber. They postulated that this increase was due to the water adsorption and moisture stability endowed by starch and fiber, resulting in higher protein concentrations in the surrounding matrix for forming the network structure (Johansson et al., 2022).

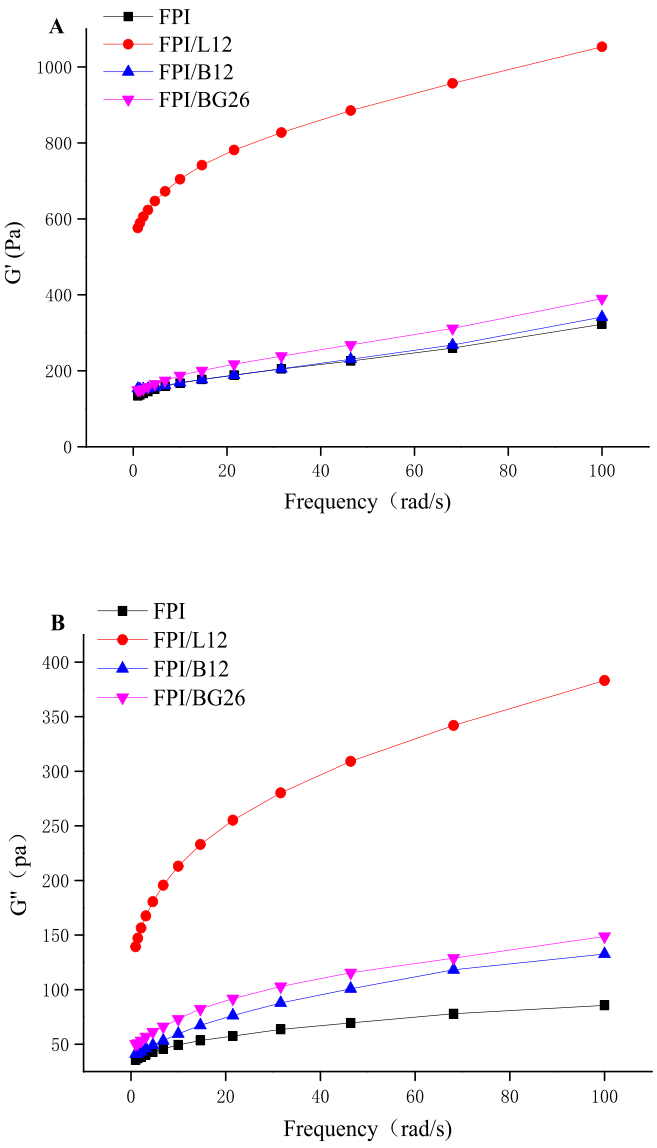

Fig. 2. Storage modulus G' (A) and loss modulus G " (B) of FPI/DX gels in the frequency sweep test.

Table 2
Effect of DXs isolated from different *Leuconostoc* strains on the hardness and WHC of FPI gels.

Gel samples	Hardness (N)	WHC (g/100 g)
FPI	0.21 ± 0.0046^{a}	61.23 ± 1.26c
FPI/L12	0.14 ± 0.0046^{c}	55.18 ± 0.48d
FPI/B12	0.18 ± 0.011^{b}	66.07 ± 0.11b
FPI/G26	0.18 ± 0.022^{b}	72.33 ± 2.27a

Values are represented as the mean ± SD (n = 3). Different superscripted letters in the same column represent significant differences ($P < 0.05$).

Impact of DX supplementation on gel microstructure

The impact of DXs on the microstructure of FPI gels was assessed based on CLSM images, as shown in Fig. 3. During CLSM analysis, the proteins labeled with Rhodamine B exhibited red color, whereas water and DX appeared black. Following the addition of DXs, varying degrees of phase separation were detected. Proteins and neutral polysaccharides are typically thermodynamically incompatible in an aqueous mixture, and phase separation usually occurs as a result of the volume exclusion effect (Monteiro & Lopes-da-Silva, 2017). DX L12 created a more open matrix structure and induced more extensive phase separation than DX

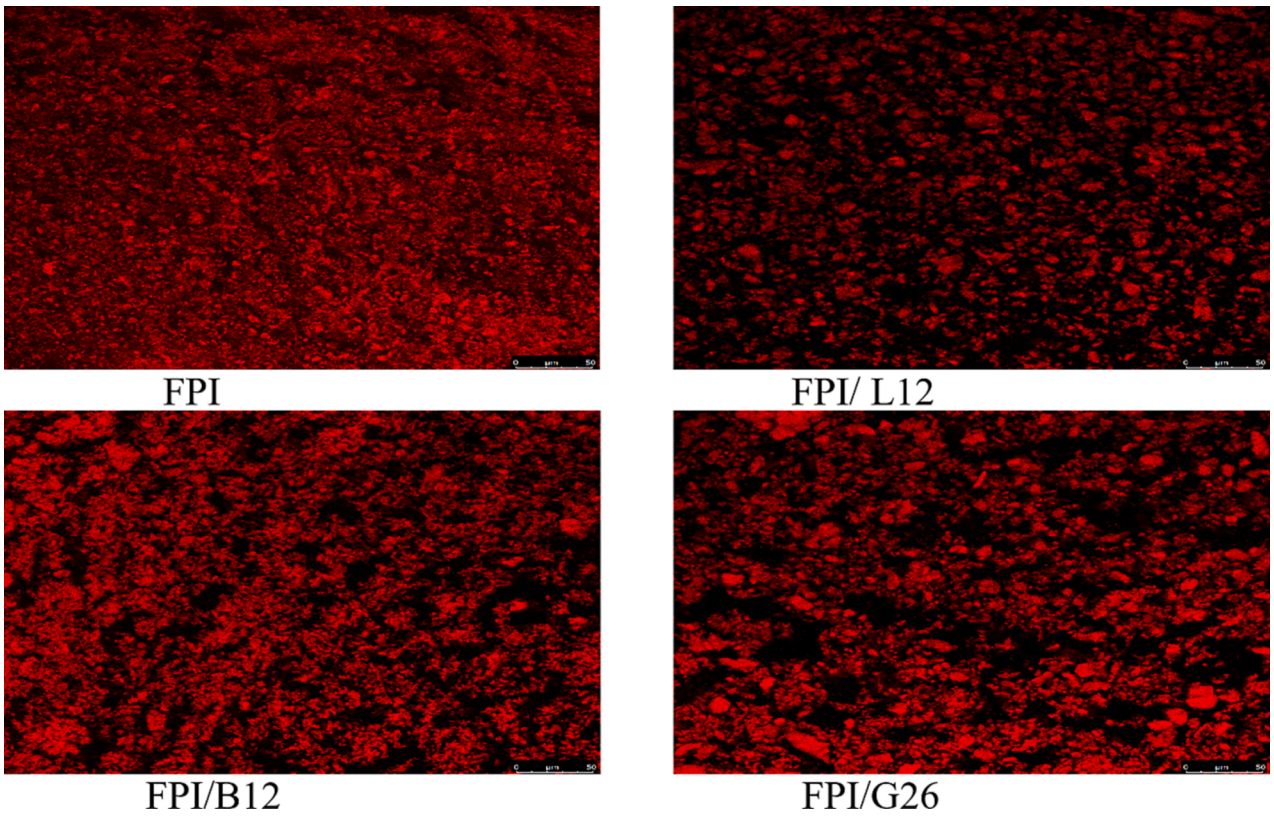

Fig. 3. CLSM micrographs (scale bar, 50 μm) of FPI and FPI/DX gels.

B12 and DX G26. One possible explanation is that DX L12, with its lowest intrinsic viscosity, may undergo self-association within each phase through its elongated chains, thus promoting phase separation. In DX B12 and DX G26, the distribution of single-unit branches along the main chain may hinder polymer self-association and cause a moderate degree of phase separation. The phase separation of the system and the water adsorption capacity of DX may jointly increase local protein concentrations for network establishment, consistent with the increase in the gel's viscoelastic moduli. In line with these findings, Monteiro et al. found that among galactomannans of similar weight-average molecular weights, the intrinsic viscosity was inversely correlated with the degree of phase separation and the viscoelastic moduli of soy protein/galactomannan gels (Monteiro et al., 2013). Moreover, the addition of galactomannan at higher concentrations resulted in more prominent phase separation in soybean protein-based gels, contributing to a marked increase in the viscoelastic moduli (Monteiro & Lopes-da-Silva, 2017). In the present study, the large void spaces (i.e., pores) in the FPI/L12 gel could be responsible for its low WHC and hardness. Similar to the present study, in a study of GDL-induced tofu gels mixed with okara, the increase in G' was also accompanied by decreased textural parameters (Lan et al., 2021). Textural properties are often governed by the inhomogeneity of the gel matrix. Meanwhile, small deformation properties are typically not as dependent on inhomogeneity and the presence of inactive fillers and are primarily governed by the continuous protein phase (Johansson et al., 2022).

Impact of DX supplementation on the intermolecular forces in FPI gels

Chemical interactions and free sulfhydryl groups

Fig. 4A shows the interaction forces among protein molecules and the free sulfhydryl content in FPI gels. The addition of DX L12 weakened the four interaction forces ($P < 0.05$), corroborating the observation of a highly porous structure in the FPI/L12 gel. Hydrogen bonds decreased significantly after DX addition ($P < 0.05$), suggesting a reduction in the role of hydrogen bonds in gel formation. The addition of DX B12 and DX G26 increased the strength of hydrophobic interactions, which was consistent with the more compact protein structures observed in the corresponding gels. The decrease in disulfide bonds and increase in free SH- content after DX addition could be ascribed to the DX-induced inhibition of disulfide bond formation during gelation. In a previous study, the inclusion of adlay starch was found to restrict the motion of protein chains by increasing the stickiness of the system, which may explain the interference of sulfhydryl-disulfide interchange (Li et al., 2019).

FTIR analysis

In the FTIR spectra of FPI gels (Fig. 4B), the absorption band in the 3600–3100 cm^{-1} band could be attributed to N—H and O—H stretching vibrations (He et al., 2021). The amide I band (1700–1600 cm^{-1}) was assigned to C═O stretching vibrations. Meanwhile, the spectral range between 800 and 1200 cm^{-1} was identified as a fingerprint area for polysaccharides (Razi et al., 2018). Interestingly, the band in the spectral range of 3600–3100 cm^{-1} shifted towards a higher wavenumber after DX addition, indicating the increased strength of hydrogen bonds (Min et al., 2022). This finding contradicted the decrease in hydrogen bonds observed in the protein solubility assay. This difference can be explained by the fact that the FTIR spectrum represents the force between protein and DX molecules, while the solubility assay examines the forces involving only protein molecules (Cortez-Trejo et al., 2022). Notably, the peak of the FPI gel at 1537 cm^{-1} shifted toward a higher wavenumber subsequent to DX addition. This was interpreted as evidence for newly formed C—N covalent bonds (Mu et al., 2020) and thus indicated the occurrence of protein glycosylation in the presence of DX.

Conclusion

DX is a commonly used natural polysaccharide produced by LAB. The aim of this study was to examine, for the first time, the influences of DXs with different branching features on the textural, rheological, and

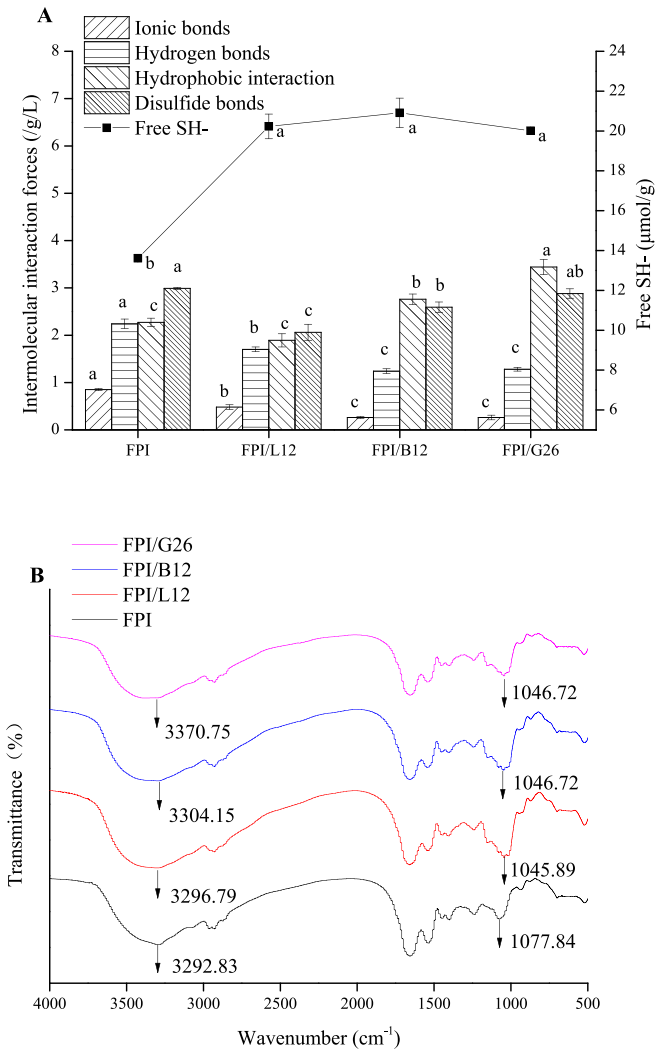

Fig. 4. Contributions of intermolecular forces and free sulfhydryl (SH-) content in FPI gels (A). FTIR spectra of the FPI and FPI/DX gels (B). Different letters for the same molecular force represent significant differences ($P < 0.05$).

microstructural properties of acid-induced FPI gels. In this study, the effects of DXs were found to be dependent on their branching patterns and intrinsic viscosities. Following DX addition, the hardness of all gels decreased and their viscoelasticity increased, and α-(1 → 3)-branched DX L12 had the most significant effect in this regard. As for gel WHC, contrasting effects were observed after DX addition, with DX L12 decreasing the WHC and the other two DXs increasing this parameter. CLSM images of the gels revealed varying degrees of phase separation after the addition of DXs. The addition of DX L12 led to extensive phase separation and created a more porous gel network, whereas the addition of DX B12 and DX G26 led to moderate phase separation and more effective protein interaction for network formation. The effects of DXs on the gel properties of FPI gels seemed to depend on the degree of phase separation and the ability of the polysaccharide to interact with water and itself. Moreover, protein interaction force analysis and FTIR spectroscopy provided more insights into the mechanisms underlying the different effects of DXs on FPI gels. This study illustrates the potential of specific DXs in modulating the acid-induced gelation of FPI, which occurs during the preparation of a wide range of food products. Future studies must explore the roles of specific DXs, produced *ex situ* and *in situ* by LAB, in modifying the properties of plant protein-based foods.

CRediT authorship contribution statement

Huihua Tang: Conceptualization, Data curation, Formal analysis, Methodology, Writing – original draft. **Junfei Chen:** Investigation, Resources. **Biqin Liu:** Investigation, Methodology. **Rong Tang:** Investigation. **Hong Li:** Resources. **Xinyi Li:** Investigation. **Ling Zou:** Formal analysis, Investigation, Resources, Writing – review & editing. **Qiao Shi:** Conceptualization, Funding acquisition, Methodology, Project administration, Writing – original draft.

Declaration of competing interest

The authors declare that they have no known competing financial interests or personal relationships that could have appeared to influence the work reported in this paper.

Data availability

Data will be made available on request.

Acknowledgments

This research was supported by the National Natural Science Foundation of China (No. 31960468).

References

Augustin, M. A., & Cole, M. B. (2022). Towards a sustainable food system by design using faba bean protein as an example. *Trends in Food Science and Technology, 125*, 1–11. https://doi.org/10.1016/j.tifs.2022.04.029

Beveridge, T., Tome, S. J., & Nakai, S. (1974). Determination of SH- and SS-Groups in Some Food Proteins Using Ellman ' Reagent. *Journal of Food Science, 39*, 49–51.

Brito-Oliveira, T. C., Bispo, M., Moraes, I. C. F., Campanella, O. H., & Pinho, S. C. (2017). Stability of curcumin encapsulated in solid lipid microparticles incorporated in cold-set emulsion filled gels of soy protein isolate and xanthan gum. *Food Research International, 102*, 759–767. https://doi.org/10.1016/j.foodres.2017.09.071

Chen, Z., Tian, Y., Zhang, W., Guang, C., Meng, X., & Mu, W. (2019). Novel Dextransucrase Gtf-DSM, Highly Similar in Sequence to Reuteransucrase GtfO, Displays Unique Product Specificity. *Journal of Agricultural and Food Chemistry, 67* (46), 12806–12815. https://doi.org/10.1021/acs.jafc.9b04252

Cortez-Trejo, M. C., Gaytán-Martínez, M., Reyes-Vega, M. L., & Mendoza, S. (2021). Protein-gum-based gels: Effect of gum addition on microstructure, rheological properties, and water retention capacity. *Trends in Food Science and Technology, 116*, 303–317. https://doi.org/10.1016/j.tifs.2021.07.030

Cortez-Trejo, M. C., Loarca-Piña, G., Figueroa-Cárdenas, J. D., Manríquez, J., & Mendoza, S. (2022). Gel properties of acid-induced gels obtained at room temperature and based on common bean proteins and xanthan gum. *Food Hydrocolloids, 132*, Article 107873. https://doi.org/10.1016/j.foodhyd.2022.107873

Dille, M. J., Knutsen, S. H., & Draget, K. I. (2022). Gels and gelled emulsions prepared by acid-induced gelation of mixtures of faba bean (Vicia faba) protein concentrate and λ-carrageenan. *Applied Food Research, 2*(2), Article 100174. https://doi.org/10.1016/j.afres.2022.100174

Dong, H., Li, Y., Jia, C., Zhang, B., Niu, M., Zhao, S., & Xu, Y. (2022). Mechanism behind the rheological property improvement of fava bean protein by the presence of dextran. *Food Hydrocolloids, 133*, Article 107907. https://doi.org/10.1016/j.foodhyd.2022.107907

Gómez-Guillén, M. C., Borderías, A. J., & Montero, P. (1997). Chemical interactions of nonmuscle proteins in the network of sardine (Sardina pilchardus) muscle gels. *Lwt - Food Science and Technology, 30*(6), 602–608. https://doi.org/10.1006/fstl.1997.0239

He, Z., Liu, C., Zhao, J., Li, W., & Wang, Y. (2021). Physicochemical properties of a ginkgo seed protein-pectin composite gel. *Food Hydrocolloids, 118*, Article 106781. https://doi.org/10.1016/j.foodhyd.2021.106781

Heperkan, Z. D., Bolluk, M., & Bülbül, S. (2020). Structural analysis and properties of dextran produced by Weissella confusa and the effect of different cereals on its rheological characteristics. *International Journal of Biological Macromolecules, 143*, 305–313. https://doi.org/10.1016/j.ijbiomac.2019.12.036

Johansson, M., Johansson, D., Ström, A., Rydén, J., Nilsson, K., Karlsson, J., Moriana, R., & Langton, M. (2022). Effect of starch and fibre on faba bean protein gel characteristics. *Food Hydrocolloids, 131*, Article 107741. https://doi.org/10.1016/j.foodhyd.2022.107741

Lan, Q., Li, L., Dong, H., Wu, D., Chen, H., Lin, D., Qin, W., Yang, W., Vasanthan, T., & Zhang, Q. (2019). Effect of soybean soluble polysaccharide on the formation of glucono-δ-lactone-induced soybean protein isolate gel. *Polymers, 11*(12), 1997. https://doi.org/10.3390/polym11121997

Lan, Q., Lin, Z., Dong, H., Wu, D., Lin, D., Qin, W., Liu, J., Yang, W., & Zhang, Q. (2021). Influence of okara with varying particle sizes on the gelling, rheological, and

microstructural properties of glucono-δ-lactone-induced tofu. *Journal of Food Science and Technology, 58*(2), 520–531. https://doi.org/10.1007/s13197-020-04563-7

Li, C., Chen, G., Ran, C. X., Liu, L., Wang, S., Xu, Y., Tan, Y., & Kan, J. (2019). Adlay starch-gluten composite gel: Effects of adlay starch on rheological and structural properties of gluten gel to molecular and physico-chemical characteristics. *Food Chemistry, 289*, 121–129. https://doi.org/10.1016/j.foodchem.2019.03.030

Li, X., Liu, Y., Li, N., Xie, D., Yu, J., Wang, F., & Wang, J. (2016). Studies of phase separation in soluble rice protein/different polysaccharides mixed systems. *Lwt- Food Science and Technology, 65*, 676–682. https://doi.org/10.1016/j.lwt.2015.08.064

Maina, N. H., Pitkänen, L., Heikkinen, S., Tuomainen, P., Virkki, L., & Tenkanen, M. (2014). Challenges in analysis of high-molar mass dextrans: Comparison of HPSEC, AsFlFFF and DOSY NMR spectroscopy. *Carbohydrate Polymers, 99*, 199–207. https://doi.org/10.1016/j.carbpol.2013.08.021

Maina, N. H., Virkki, L., Pynnönen, H., Maaheimo, H., & Tenkanen, M. (2011). Structural analysis of enzyme-resistant isomaltooligosaccharides reveals the elongation of α-(1→3)-linked branches in weissella confusa dextran. *Biomacromolecules, 12*(2), 409–418. https://doi.org/10.1021/bm1011536

Makri, E. A., Papalamprou, E. M., & Doxastakis, G. I. (2006). Textural properties of legume protein isolate and polysaccharide gels Eleousa. *Journal of the Science of Food and Agriculture, 86*, 1855–1862. https://doi.org/10.1002/jsfa

Martineau-Côté, D., Achouri, A., Karboune, S., & L'Hocine, L. (2022). Faba Bean: An Untapped Source of Quality Plant Proteins and Bioactives. *Nutrients, 14*(8), 1–27. https://doi.org/10.3390/nu14081541

Mende, S., Jaros, D., & Rohm, H. (2020). Dextran modulates physical properties of rennet-induced milk gels. *International Journal of Food Science and Technology, 55*(4), 1407–1415. https://doi.org/10.1111/ijfs.14288

Mende, S., Peter, M., Bartels, K., Dong, T., Rohm, H., & Jaros, D. (2013). Concentration dependent effects of dextran on the physical properties of acid milk gels. *Carbohydrate Polymers, 98*(2), 1389–1396. https://doi.org/10.1016/j.carbpol.2013.07.072

Min, C., Ma, W., Kuang, J., Huang, J., & Xiong, Y. L. (2022). Textural properties, microstructure and digestibility of mungbean starch–flaxseed protein composite gels. *Food Hydrocolloids, 126*, Article 107482. https://doi.org/10.1016/j.foodhyd.2022.107482

Monteiro, S. R., & Lopes-da-Silva, J. A. (2017). Effect of the molecular weight of a neutral polysaccharide on soy protein gelation. *Food Research International, 102*, 14–24. https://doi.org/10.1016/j.foodres.2017.09.066

Monteiro, S. R., Rebelo, S., da Cruz e Silva, O. A. B., & Lopes-da-Silva, J. A. (2013). The influence of galactomannans with different amount of galactose side chains on the gelation of soy proteins at neutral pH. *Food Hydrocolloids, 33*(2), 349–360. https://doi.org/10.1016/j.foodhyd.2013.04.012

Mu, Y., Sun, J., Obadi, M., Chen, Z., & Xu, B. (2020). Effects of saccharides on the rheological and gelling properties and water mobility of egg white protein. *Food Hydrocolloids, 108*, Article 106038. https://doi.org/10.1016/j.foodhyd.2020.106038

Pang, Z., Luo, Y., Li, B., Zhang, M., & Liu, X. (2020). Effect of different hydrocolloids on tribological and rheological behaviors of soymilk gels. *Food Hydrocolloids, 101*, Article 105558. https://doi.org/10.1016/j.foodhyd.2019.105558

Pang, Z., Xu, R., Zhu, Y., Li, H., Bansal, N., & Liu, X. (2019). Comparison of rheological, tribological, and microstructural properties of soymilk gels acidified with glucono-δ-lactone or culture. *Food Research International, 121*, 798–805. https://doi.org/10.1016/j.foodres.2018.12.062

Rahate, K. A., Madhumita, M., & Prabhakar, P. K. (2021). Nutritional composition, anti-nutritional factors, pretreatments-cum-processing impact and food formulation potential of faba bean (Vicia faba L.): A comprehensive review. Lwt-Food. *Science and Technology, 138*, Article 110796. https://doi.org/10.1016/j.lwt.2020.110796

Razi, M. S., Motamedzadegan, A., Shahidi, A., & Rashidinejad, A. (2018). The effect of basil seed gum (BSG) on the rheological and physicochemical properties of heat-induced egg albumin gels. *Food Hydrocolloids, 82*, 268–277. https://doi.org/10.1016/j.foodhyd.2018.01.013

Rizzello, C. G., Coda, R., Wang, Y., Verni, M., Kajala, I., Katina, K., & Laitila, A. (2019). Characterization of indigenous Pediococcus pentosaceus, Leuconostoc kimchii, Weissella cibaria and Weissella confusa for faba bean bioprocessing. *International Journal of Food Microbiology, 302*, 24–34. https://doi.org/10.1016/j.ijfoodmicro.2018.08.014

Serrano, S., Rincón, F., & García-Olmo, J. (2013). Cereal protein analysis via Dumas method: Standardization of a micro-method using the EuroVector Elemental Analyser. *Journal of Cereal Science, 58*(1), 31–36. https://doi.org/10.1016/j.jcs.2013.04.006

Spotti, M. J., Loyeau, P. A., Marangón, A., Noir, H., Rubiolo, A. C., & Carrara, C. R. (2019). Influence of Maillard reaction extent on acid induced gels of whey proteins and dextrans. *Food Hydrocolloids, 91*, 224–231. https://doi.org/10.1016/j.foodhyd.2019.01.020

Tang, H., Li, X., Chen, J., Liu, B., Tang, R., Chen, Y., Li, H., Zou, L., & Shi, Q. (2023). Effects of Dextran on the Gel Properties of Faba Bean Protein Isolates Prepared Using Different Processes. *Gels, 9*(12), 972.

Ullah, I., Hu, Y., You, J., Yin, T., Xiong, S., & Din, Z. (2019). Influence of okara dietary fiber with varying particle sizes on gelling properties, water state and microstructure of tofu gel. *Food Hydrocolloids, 89*, 512–522. https://doi.org/10.1016/j.foodhyd.2018.11.006

Xu, Y., Coda, R., Shi, Q., Tuomainen, P., Katina, K., & Tenkanen, M. (2017). Exopolysaccharides Production during the Fermentation of Soybean and Fava Bean Flours by Leuconostoc mesenteroides DSM 20343. *Journal of Agricultural and Food Chemistry, 65*(13), 2805–2815. https://doi.org/10.1021/acs.jafc.6b05495

Xu, Y., Pitkänen, L., Maina, N. H., Coda, R., Katina, K., & Tenkanen, M. (2018). Interactions between fava bean protein and dextrans produced by Leuconostoc pseudomesenteroides DSM 20193 and Weissella cibaria Sj 1b. *Carbohydrate Polymers, 190*, 315–323. https://doi.org/10.1016/j.carbpol.2018.02.082

Yang, Y., Peng, Q., Guo, Y., Han, Y., Xiao, H., & Zhou, Z. (2015). Isolation and characterization of dextran produced by Leuconostoc citreum NM105 from manchurian sauerkraut. *Carbohydrate Polymers, 133*, 365–372. https://doi.org/10.1016/j.carbpol.2015.07.061

Zhao, C., Miao, Z., Qi, Q., Zheng, Q., Mao, Y., Chu, Z., Zhang, H., Xu, X., Zheng, M., & Liu, J. (2023). Interactions of soy protein isolate with common and waxy corn starches and their effects on acid-induced cold gelation properties of complexes. *Food Chemistry: X, 18*, Article 100671. https://doi.org/10.1016/j.fochx.2023.100671

Zheng, H., Beamer, S. K., Matak, K. E., & Jaczynski, J. (2019). Effect of κ-carrageenan on gelation and gel characteristics of Antarctic krill (Euphausia superba) protein isolated with isoelectric solubilization/precipitation. *Food Chemistry, 278*, 644–652. https://doi.org/10.1016/j.foodchem.2018.11.080

Zheng, L., Teng, F., Wang, N., Zhang, X., Regenstein, J. M., & Liu, J. (2019). applied sciences Addition of Salt Ions before Spraying Improves Heat- and Cold-Induced Gel Properties of Soy Protein Isolate (SPI). *Applied Sciences, 9*(6), 1076. https://doi.org/10.3390/app9061076